

# The Parity Non-Conserving ${}^3P_0 - {}^1P_1$ E1 Transition Amplitude of the Atomic Yb

Angom Dilip Singh\*

*Physical Research Laboratory, Navarangpura, Ahmedabad-9,  
INDIA*

Bhanu Pratap Das†

*Non-Accelerator Particle Physics Group,  
Indian Institute of Astrophysics,  
Koramangala, Bangalore - 34,  
INDIA*

The atomic parity non-conservation(PNC) experiments has reached accuracies which have important implications for physics beyond the standard model. An optical rotation experiment to measure the atomic PNC of the  ${}^3P_1(6s6p) - {}^1P_1(6s6p)$  in Yb was proposed recently[1]. Our screened electron-electron coulomb potential multi-configuration Dirac-Fock calculation of th PNC induced E1 transition amplitude of this transition  $E1_{\text{PNC}} = -96.0 \times 10^{-11} iea_0(-Q_W/N)$  of  ${}^{171}\text{Yb}$  is more than two orders of magnitude larger than  $E1_{\text{PNC}}(6s-7s) = -0.8991 \times 10^{-11} iea_0(-Q_W/N)$  of  ${}^{133}\text{Cs}$ .

## I. INTRODUCTION

The nuclear weak charge  $Q_W$  of an atom is a parameter of the atomic PNC arising from the nucleon-electron vector axial vector interaction. It is possible to extract  $Q_W$  by measuring the PNC induced electric dipole transition amplitude  $E1_{\text{PNC}}$  and combining it with atomic theory calculations. The  $E1_{\text{PNC}}$  of the  ${}^{133}\text{Cs}$   $6s - 7s$  transition has been measured to very high accuracy[2]. The  $Q_W$  of  ${}^{133}\text{Cs}$  obtained from the experimental data after combining with the atomic theory calculations[3, 4] was further refined to  $72.06(28)_{\text{expt}}(34)_{\text{theor}}$  after the measurement of the  $6s - 7s$  transition polarizability[5]. This has a  $2.5\sigma$  deviation from the predictions of the standard model  $Q_W = 73.20(13)$ [6]. The uncertainty of the experiment results and atomic theory calculations are estimated at .35% and 1% respectively. This indicate the possibility of improving the results further by reducing the atomic theory uncertainty.

The recent atomic theory calculations which treat the Breit interaction more rigorously have introduced corrections of .9%[7], .6%[8] and .4%[9] to  $Q_W$  of  ${}^{133}\text{Cs}$ . The variation of the results is due to the difference of the calculation methods and many-body effects included. The uncertainties of these calculations are estimated at 1%. Considering the unique implications of the parameters obtained from the atomic PNC phenomena to the physics beyond the standard model, it is desirable to reduce the atomic theory uncertainties and also confirm the  ${}^{133}\text{Cs}$  results using other atoms.

An important criteria of choosing a candidate atom is the  $Z^3\alpha$  scaling of the PNC interaction, which indicates the advantage of choosing high  $Z$  atom. The  ${}^1S_0 - {}^3D_1$  transition of atomic Yb( $Z = 70$ ), which has been stud-

ied theoretically[10, 11, 12, 13] and experimentally[15, 27] in detail is a promising candidate of the ongoing and future atomic PNC experiments. This transition is a suitable choice due to the nearly degenerate  ${}^3D_1(5d6s)(24489\text{cm}^{-1})$  and  ${}^1P_1(6s6p)(25068\text{cm}^{-1})$ , which can enhance the PNC mixing. The PNC mixing enhancement between this pair of levels can also be exploited in the  ${}^3P_0 - {}^1P_1$  transition.

The  ${}^3P_0 - {}^1P_1$  transition was proposed for atomic PNC experiment in a recent work[1] and estimates  $E1_{\text{PNC}} \approx 7 \times 10^{-10} ea_0$  which is almost one order of magnitude larger than that of  ${}^{133}\text{Cs}$   $E1_{\text{PNC}} \approx 8 \times 10^{-11} ea_0$ . The use of the metastable state  ${}^3P_0$  as the initial state offers the possibility of separating only the atomic density dependent plane of polarization rotation angle from the wavelength dependent systematic errors. This is expected to better the results obtained from the Stark-interference experiments, where the use of the high intensity laser fields limits the statistical precision due to the light shift.

In this paper we have investigated the  $E1_{\text{PNC}}$  of the  ${}^3P_{0,1} - {}^1P_1$  transition using multi-configuration Dirac-Fock method. The atomic theory calculations are necessary to extract the nuclear weak charge  $Q_W$  from the experimental value of  $E1_{\text{PNC}}$ . To check the accuracy of the atomic calculations we also study the transition properties and hyper fine structure constants. All the calculations are in atomic units ( $\hbar = e = m_e = 1$ ).

## II. THE METHOD OF CALCULATION

The nuclear spin-independent atomic PNC arises from the axial-vector vector electron-nucleon interaction component of the neutral weak current interaction between the electrons and nucleons of an atom. The interaction is mediated by  $Z_0$  bosons, which is a prediction of the electron-weak unification. The effective form of the interaction Hamiltonian can be obtained by treating the

\*Electronic address: angom@prl.ernet.in

†Electronic address: das@iiap.ernet.in

nuclear part non-relativistically

$$H_{\text{PNC}}^{\text{NSI}} = \frac{G_F}{\sqrt{8}} Q_W \gamma_5 \rho_{\text{nuc}}(r), \quad (2.1)$$

where  $G_F$  is the Fermi coupling constant,  $\gamma_5$  is the Dirac matrix and  $\rho_{\text{nuc}}$  is the nuclear density. The PNC induced  $E1$  transition amplitude between the initial and final states  $|\Psi_i\rangle$  and  $|\Psi_f\rangle$  is

$$E1_{\text{PNC}} = \sum_I \left[ \frac{\langle \Psi_f | \mathbf{D} | \Psi_I \rangle \langle \Psi_I | H_{\text{PNC}}^{\text{NSI}} | \Psi_i \rangle}{E_i - E_I} + \frac{\langle \Psi_f | H_{\text{PNC}}^{\text{NSI}} | \Psi_I \rangle \langle \Psi_I | \mathbf{D} | \Psi_i \rangle}{E_f - E_I} \right], \quad (2.2)$$

where  $|\Psi_I\rangle$  are the intermediate states which are opposite in parity to  $|\Psi_i\rangle$  and  $|\Psi_f\rangle$ , and  $E_i$ ,  $E_f$  and  $E_I$  are the energies of the states.

The numerator of (2.2) has  $H_{\text{PNC}}^{\text{NSI}}$ , effective only within the nuclear region due to the nuclear density  $\rho_{\text{nuc}}(r)$  and the dipole  $\mathbf{D} = -\mathbf{r}$  in length gauge, which has significant contribution from the large radial range. And the energies in the denominator has large contribution from the mid radial range where the electron density is high. The calculation of the  $E1_{\text{PNC}}^{\text{NSI}}$  require atomic state functions which are accurate over all radial ranges.  $E1_{\text{PNC}}$  can be calculated once the atomic wave-functions are known.

### A. Wave-function Calculation

A method suitable for rare earth atoms which has large configuration mixing is the multi-configuration Dirac-Fock (MCDF), which is the relativistic adaptation of the multi-configuration Hartree-Fock. The MCDF approximates an atomic state function  $|\Gamma P J M\rangle$  as a linear combination of configuration state functions (CSF)  $|\gamma P J M\rangle$ , which are again a linear combination of Slater determinants. Where  $P$ ,  $J$  and  $M$  are the parity, total angular momentum and magnetic quantum numbers respectively, and  $\Gamma$  and  $\gamma$  are the additional quantum numbers required to defined the ASF and CSFs uniquely. Then

$$|\Gamma_i P J M\rangle = \sum_r c_{r\Gamma_i} |\gamma_r P J M\rangle, \quad (2.3)$$

where  $c_{r\Gamma_i}$  are the coefficients of the CSFs. The energy functional is defined using a set of ASFs which mix strongly and the Dirac-Coulomb Hamiltonian

$$H_{\text{DC}} = \sum_i^N \left[ c\alpha_i \cdot \mathbf{p}_i + \beta_i c^2 - \frac{Z}{r_i} \right] + \sum_{i<j}^N \frac{1}{r_{ij}}, \quad (2.4)$$

where  $\alpha_i$  and  $\beta_i$  are the Dirac matrices,  $\mathbf{p}_i$  is the momentum and  $N$  is the number of electrons. The orbitals are then generated variationally. The orbitals from the negative continuum are also the solutions of such a method, however only the bound states can be chosen by imposing the boundary condition that the orbitals  $\psi(\mathbf{r}) \rightarrow 0$  as

$r \rightarrow \infty$ . Choosing the ASFs contributing to the valence-valence correlation effects, the orbitals captures important correlation effects.

Though MCDF method can represent the valence-valence correlation, it is not a suitable method to calculate core-valence and core-core correlation effects. A large number of CSFs is required to represent these correlation effects, which is computationally difficult as self consistent field method like MCDF is not suitable for a calculation involving large CSF spaces. However, these correlation effects can be calculated using configuration interaction(CI) using a set of virtual orbitals generated from the MCDF potential.

A large set of CSFs is required in the CI calculation to represent all classes of correlation effects. A more efficient method is to model it using the most important CSFs and modifying the form of the electron-electron Coulomb interaction potential as

$$\frac{1}{r_{12}} = \sum_K \alpha_K \frac{r_{<}^K}{r_{>}^{K+1}} \mathbf{C}_K(1) \cdot \mathbf{C}_K(2), \quad (2.5)$$

where  $\alpha_K$  are the constants that modifies the  $K^{\text{th}}$  multipole of the inter electron Coulomb interaction potential. The suitable values of these constants can be obtained by matching properties like excitation energies calculated using this potential with the experimental data. The earlier calculations have shown that, this approach can reproduce the experimental data to very good agreement[10, 16]. The values of  $\alpha$  are chosen such that  $0 < \alpha_K < 1$ . and for consistency the screening parameters are used in the MCDF calculations to generate the orbitals.

### B. Properties Calculation

The most important transition properties like oscillator strength, life time, polarizability, etc arise from the electric dipole transition. And all of these depend on the reduce matrix elements of the electric dipole operator. Consider the initial and final states of the atom  $|\Psi_i\rangle$  and  $|\Psi_f\rangle$ , then from Wigner-Eckert theorem

$$D_{if} = \sum_q \begin{pmatrix} J_f & 1 & J_i \\ -m_f & q & m_i \end{pmatrix} (-1)^{(J_f - m_f)} \langle \Psi_f || D || \Psi_i \rangle, \quad (2.6)$$

where  $J_f$  and  $J_i$  are the total angular momenta of the final and initial states,  $m_f$  and  $m_i$  are the magnetic quantum number of the final and initial states, and  $q$  is the component of the dipole operator.  $\langle \Psi_f || D || \Psi_i \rangle = D_{fi}$  is the reduced matrix element and it is independent of geometry. The reduced matrix elements can be expressed in terms of the ASFs as

$$D_{fi} = \langle \Gamma_f P_f J_f || D || \Gamma_i P_i J_i \rangle \quad (2.7)$$

$$= \sum_{rs} c_{r\Gamma_f} c_{s\Gamma_i} \langle \gamma_r P_f J_f || D || \gamma_s P_i J_i \rangle. \quad (2.8)$$

The oscillator strength of the transition  $|\Psi_i\rangle - |\Psi_f\rangle$  is

$$f_{fi} = \frac{2\Delta E}{3(2J_f + 1)} |D_{fi}|^2, \quad (2.9)$$

where  $\Delta E = E_f - E_i$ . The independent particle approximation of the inter-electron electromagnetic interaction implies that it is not gauge invariant. However, the gauge invariance is restored if the inter-electron electromagnetic interaction is represented completely by including the correlation effects correctly. The agreement of the dipole matrix elements or transition properties calculated in different gauges indicate the completeness of the correlation effects included, which can also be interpreted as the accuracy of the wave-functions.

The hyperfine constants are the measure of the strength of the electron-nucleus parity allowed electromagnetic multipole interactions. The general form of the interaction Hamiltonian is

$$H_{\text{hfs}} = \sum_k \mathbf{T}^{(k)} \cdot \mathbf{M}^{(k)}, \quad (2.10)$$

where  $\mathbf{T}^{(k)}$  and  $\mathbf{M}^{(k)}$  are spherical tensor operators of rank  $k$  in the electron and nuclear space respectively. These represent the electromagnetic multipoles. The  $k = 1$  and  $2$  corresponding to the magnetic dipole and electric quadrupole respectively are the most important. The atomic states are then the eigenstates of the total angular momentum

$$\mathbf{F} = \mathbf{I} + \mathbf{J}, \quad (2.11)$$

where  $\mathbf{I}$  is the nuclear spin. The shift in energy due to the magnetic dipole and electric quadrupole hyperfine interactions of the atomic state  $|\gamma_I \gamma_J I J F M_f\rangle$  are

$$W_{M1}(J, J) = \frac{1}{2} A_J C$$

$$W_{E2}(J, J) = B_J \frac{\frac{3}{4} C(C+1) - I(I+1)J(J+1)}{2I(2I-1)J(2J-1)}$$

where  $C = F(F+1) - J(J+1) - I(I+1)$ , and  $A_J$  and  $B_J$  are the magnetic dipole and electric quadrupole hyperfine constants respectively. These are defined as

$$A_J = \frac{\mu_I}{I} \frac{1}{[J(J+1)(2J+1)]^{\frac{1}{2}}} \langle \gamma_J J || \mathbf{T}^{(1)} || \gamma_J J \rangle$$

$$B_J = 2Q \left[ \frac{2J(2J-1)}{(2J+1)(2J+2)(2J+3)} \right]^{\frac{1}{2}} \langle \gamma_J J || \mathbf{T}^{(2)} || \gamma_J J \rangle$$

where  $\mu_I$  and  $Q$  are the nuclear magnetic dipole and electric quadrupole moments.

### III. RESULTS

#### A. Screened Coulomb Potential

The low-lying levels of the Yb are given in the Fig 1. The  $H_{\text{PNC}}$  mixing between the  $|^1P_1(6s6p)\rangle$  and

$|^3D_1(5d6s)\rangle$  reduces to mixing between  $5d$  and  $6p$  at the single particle level, which is negligible as  $5d$  is almost zero in the nuclear region. However,  $6s$  and  $6p$  mixing can occur through the mixing  $\langle ^3D_1(5d6s) | H_{\text{PNC}} | 5d6p \rangle$ , which arises due to the strong configuration mixing between  $|6s6p\rangle$  and  $|5d6p\rangle$ . So the most important contribution to the  $E_{\text{PNC}}(^3P_0 - ^1P_1)$  transition amplitude is

$$\frac{\langle ^1P_1(6s6p) | D | 5d6p \rangle \langle 5d6p | H_{\text{PNC}} | ^3P_0(6s6p) \rangle}{E_{|^3P_0(6s6p)\rangle} - E_{|^5d5p\rangle}} + \frac{\langle ^1P_1(6s6p) | H_{\text{PNC}} | 5d6p \rangle \langle 5d6p | D | ^3P_0(6s6p) \rangle}{E_{|^1P_1(6s6p)\rangle} - E_{|^5d5p\rangle}}.$$

This indicates that the choice of  $|^3P_1(6s6p)\rangle$  as initial state offers the possibility of non-zero contribution from the leading configurations to the normal and conjugate terms. Whereas the largest contribution to the  $E_{\text{PNC}}(^1S_0(6s^2) - ^1P_1(6s6p))$  is

$$\frac{\langle ^1P_1(6s6p) | D | 5d6p \rangle \langle 5d6p | H_{\text{PNC}} | ^1S_0(6s^2) \rangle}{E_{|^1S_0(6s6p)\rangle} - E_{|^5d5p\rangle}}, \quad (3.1)$$

the conjugate term does not contribute as  $|5d6p\rangle$  is double excitation with respect to  $|^1S_0(6s^2)\rangle$ .

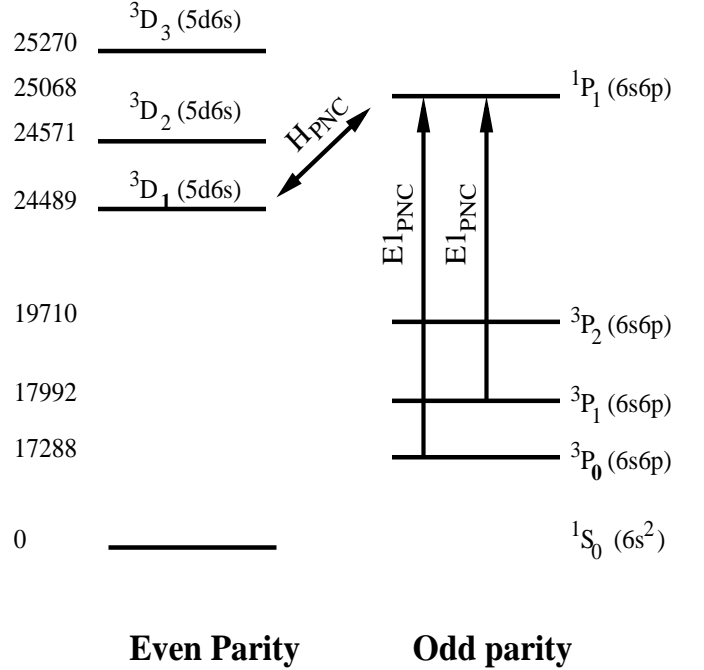


FIG. 1: The low-lying levels of atomic Yb. The double arrow represents the  $H_{\text{PNC}}$  mixing and single arrow represents the transitions of interest for  $E_{1\text{PNC}}$  measurement.

All the calculations are done using GRASP2[17] package. The choice of the screening parameters  $\alpha_s$  and the dependence of the excitation energies on these parameters are discussed in an earlier work[10, 16]. The values of the  $\alpha_K$ s which can give excitation energies very close

to the experimental data are  $\alpha_0 = 0.997$ ,  $\alpha_1 = 0.667$ ,  $\alpha_2 = 0.980$  and rest are set to unity. The even and odd parity CSF space consist of the following non-relativistic configurations:

Even parity

$$\begin{aligned} & (5p^6 4f^{14}) (6s^2 + 5d6s + 5d^2 + 6p^2) \\ & + (5p^6 4f^{13}) (6s^2 6p + 5d^2 6p + 5d6s6p) \\ & + (5p^5 4f^{14}) (6s^2 6p + 5d^2 6p + 5d6s6p) \end{aligned}$$

Odd parity

$$\begin{aligned} & (5p^6 4f^{14}) (6s6p + 5d6p) \\ & + (5p^6 4f^{13}) (5d^2 6s + 5d6s^2 + 6s6p^2 + 5d6p^2) \\ & + (5p^5 4f^{14}) (5d^2 6s + 5d6s^2 + 6s6p^2 + 5d6p^2) \end{aligned}$$

The configuration space is chosen to represent the important valence-valence and core-valence correlation effects. The excitation energies calculated using these choices of  $\alpha_K$ s and configurations are given in Table I. For a comparative study we have also calculated

TABLE I: The excitation energies of the low-lying levels in  $cm^{-1}$

Level	Expt. data	Theory
$^3P_1(6s6p)$	17992	17651
$^3P_2(6s6p)$	19710	19855
$^3D_1(5d6s)$	24489	24467
$^1P_1(6s6p)$	25068	25024

$E1_{PNC}(^3P_1(6s6p) - ^1P_1(6s6p))$ . However  $|^3P_1(6s6p)\rangle$  can decay to the ground state  $|^1S_0(6s^2)\rangle$  by magnetic quadrupole transition. Where as  $|^3P_0(6s6p)\rangle - |^1S_0(6s^2)\rangle$  is highly forbidden. The calculated values of reduced matrix element of  $E1_{PNC}$  are given in Table II. For com-

TABLE II: The  $E1_{PNC}$  reduced matrix elements of atomic  $^{171}\text{Yb}(I = 1/2)$  in units of  $iea_0(-Q_W/N) \times 10^{-11}$ .

Transition	$  E1_{PNC}  $
$^1S_0(6s^2) - ^3D_1(5d6s)$	77.8
$^3P_1(6s6p) - ^1P_1(6s6p)$	-71.7
$^3P_0(6s6p) - ^1P_1(6s6p)$	-96.0

parison  $||E1_{PNC}(^1S_0(6s^2) - ^3D_1(5d6s))||$  is also included in the table. The  $||E1_{PNC}||$  of atoms and ions which has been studied and calculated recently are given in Table III. The comparison of the  $E1_{PNC}$  transition amplitudes indicates that the  $^3P_0(6s6p) - ^1P_1(6s6p)$  transition of Yb is the largest.

## B. MCDF Calculations

The occupied orbitals  $(1-6)s$ ,  $(2-5)p$ ,  $(3-4)d$  and  $4f$ , and the valence orbitals  $6s$ ,  $5d$  and  $6p$  are gener-

TABLE III:  $E1_{PNC}$  of recently studied and calculated atomic/ionic transitions. These are given in units of  $iea_0(-Q_W/N) \times 10^{-11}$

Atom/ion	Z	N	Transition		$E1_{PNC}$
			Initial state	final state	
Cs	55	78	$ 6s_{1/2}\rangle$	$ 7s_{1/2}\rangle$	-0.8991(36) <sup>a</sup>
Cs	55	78	$ 6s_{1/2}\rangle$	$ 5d_{3/2}\rangle$	3.75 <sup>b</sup>
Ba <sup>+</sup>	55	82	$ 6s_{1/2}\rangle$	$ 5d_{3/2}\rangle$	2.17 <sup>b</sup>
Yb	70	101	$ ^1S_0(6s^2)\rangle$	$ ^3D_1(5d6s)\rangle$	79.38 <sup>c</sup>
Tl	81	124	$ 6p_{1/2}\rangle$	$ 6p_{3/2}\rangle$	66.7 ± 1.7 <sup>d</sup>
Fr	87	136	$ 7s_{1/2}\rangle$	$ 6d_{3/2}\rangle$	57.1 <sup>b</sup>
Ra	88	139	$ ^1S_0(7s^2)\rangle$	$ ^3D_1(7s6d)\rangle$	77.0 <sup>e</sup>
Ra	88	135	$ ^1S_0(7s^2)\rangle$	$ ^3D_1(7s6d)\rangle$	76.0 <sup>e</sup>
Ra <sup>+</sup>	87	135	$ 7s_{1/2}\rangle$	$ 6d_{3/2}\rangle$	42.9 <sup>b</sup>

<sup>a</sup>See ref[7]

<sup>b</sup>See ref[18]

<sup>c</sup>See ref[10]

<sup>d</sup>See ref[19]

<sup>e</sup>see ref[20]

ated by a sequence of MCDF calculations and non of the orbitals are frozen in each of the calculations. The non-relativistic configurations of the final calculation of the sequence are:  $6s^2$ ,  $6p^2$ ,  $5d6s$ ,  $5d^2$ ,  $6s6p$  and  $5d6p$ . These orbitals are generated spectroscopic, that is the number of nodes satisfy the central field condition. This selection of non-relativistic configurations include the leading configurations of the  $^3P_1(6s6p)$ ,  $^3D_1(5d6s)$  and  $^1P_1(6s6p)$  levels, and the configurations which mix strongly with these. The levels obtained as a result of the MCDF calculation are given in the column MCDF1 of TableIV. The

TABLE IV: The Yb levels in units of  $cm^{-1}$  calculated using MCDF method with the leading and next leading configurations

Levels	Excitation Energies(E)		
	Expt	MCDF1	MCDF2
$^3P_0$	17288	13428	13535
$^3P_1$	17992	14119	14234
$^3P_2$	19710	15644	15808
$^3D_1$	24489	25458	24784
$^3D_2$	24571	25507	24802
$^3D_3$	25270	25591	24844
$^1P_1$	25068	24990	25078

calculated  $E(MCDF)$  differ from the experimental data in the range 0.3% – 22.0% and the sequence is incorrect as  $^1P_1$  lies below the  $^3D_J$ . A correct sequence of the levels can be obtained by saturating the valence correlation effects by including the virtual orbitals  $6d$  and  $6f$  generated as correlation orbitals. The results of the calculation are give in column MCDF2 of TableIV. The  $^3D_J$  and  $^1P_1$  are in good agreement with the experimental data and

the  $^1P_1$  lies above  $^3D_1$  and  $^3D_2$  levels. However, it is also above  $^3D_3$ , which is in disagreement with the experimental data. This indicates that the correlation orbitals  $6d$  and  $6f$  lower the  $^3D_J$  levels but has little effect on the  $^3P_J$  and  $^1P_1$  levels.

The MCDF calculation captures the important valence-valence correlation effects. However, it is not suitable to capture the core-valence and core-core correlation effects, which require a large number of CSFs. CI calculations within the CSF space having excitations from the core and valence shells to the virtual can capture these correlation effects. The virtual orbitals required for the CI calculation is generated in layers, where one layer is a set of orbitals of  $s$ ,  $p$ ,  $d$ ,  $f$  and  $g$  symmetries having same principal quantum number. Higher angular momentum orbitals  $h$  and above are not included in the calculation. Each layer is generated by an MCDF-EOL calculation of the CSFs used in the previous calculation and the CSFs obtained by single excitation from the configurations  $6s^2$ ,  $5d6s$ ,  $6s6p$ ,  $6p^2$ ,  $6p6f$  and  $5d6p$ .

TABLE V: The excitation energies of the low-lying levels and the magnetic hyperfine structure constants.

Level	Excitation energies		Hyperfine Constant A	
	Expt	Theory	Expt	Theory
$^3P_0$	17288	15693		
		17282 <sup>a</sup>		
		17359 <sup>b</sup>		
$^3P_1$	17992	16370	-1094.0(7) <sup>c</sup>	-1065
		17997 <sup>a</sup>		-1094 <sup>a</sup>
		18089 <sup>b</sup>		
$^3P_2$	19710	17989	-738 <sup>d</sup>	-747
		19750 <sup>a</sup>		-745 <sup>a</sup>
		19836 <sup>b</sup>		
$^3D_1$	24489	23468	563 <sup>c</sup>	601
		24441 <sup>a</sup>		596 <sup>a</sup>
		24936 <sup>b</sup>		
$^3D_2$	24571	23567	-362(2) <sup>c</sup>	-307
		24697 <sup>a</sup>		-351 <sup>a</sup>
		25180 <sup>b</sup>		
$^3D_3$	25270	23744	-430(1) <sup>c</sup>	-454
		25247 <sup>a</sup>		-420 <sup>a</sup>
		25676 <sup>b</sup>		
$^1P_1$	25068	24430	59 <sup>d</sup>	152
		25074 <sup>a</sup>		191 <sup>a</sup>
		27271 <sup>b</sup>		

<sup>a</sup>See ref[21]

<sup>b</sup>See ref[22]

<sup>c</sup>See ref[23]

<sup>d</sup>See ref[24]

The results of a CI calculation within the CSF space spanned by all possible excitations from the valence shells and single excitations from the core-shells  $5s$ ,  $5p$  and  $4f$

TABLE VI:

	$^3P_0(6s6p)$	$^3P_1(6s6p)$	$^1P_1(6s6p)$
$^1S_0(6s^2)$		0.51	4.98
		0.54(8) <sup>a</sup>	4.40(80) <sup>a</sup>
		0.44 <sup>b</sup>	4.44(80) <sup>b</sup>
		0.549(4) <sup>c</sup>	4.89(80) <sup>c</sup>
		0.553(13) <sup>f</sup>	4.13(10) <sup>f</sup>
			4.02 <sup>g</sup>
			4.26 <sup>h</sup>
$^3D_1(5d6s)$	3.03	2.64	0.28
	2.61(10) <sup>a</sup>	2.26(10) <sup>a</sup>	0.27(10) <sup>a</sup>
		2.2(1) <sup>d</sup>	0.24 <sup>b</sup>

<sup>a</sup>See ref[11]

<sup>b</sup>See ref[25]

<sup>c</sup>See ref[26]

<sup>d</sup>See ref[27]

<sup>e</sup>See ref[15]

<sup>f</sup>See ref[28]

<sup>g</sup>See ref[29]

<sup>h</sup>See ref[30]

with respect to the  $6s^2$ ,  $5d6s$ ,  $6s6p$ ,  $6p^2$ ,  $6p6f$  and  $5d6p$  are given in TableV. The results of earlier calculations are also given in the table. The sequence of the excitation energies are correct but the deviation from the experimental values is still large. However, the level  $^1P_1$  is better than the coupled-cluster results and the hyperfine constant of the same level is in better agreement with the experimental data. The important reduced matrix elements of the electric dipole are given in the Table:VI.

The  $E1_{\text{PNC}}$  calculated using the theoretical results is  $-86.01 \times 10^{-11}i(-Q_W/N)ea_0$ . The important contributions are from the intermediate states  $^3D_1(5d6s)$  and  $^1S_0(6s^2)$ , each of these yield  $-90.62 \times 10^{-11}(-Q_W/N)ea_0$  and  $24.74 \times 10^{-11}i(Q_W/N)ea_0$  respectively. The cancellation due to the  $^1S_0(6s^2)$  is large but is nearly compensated by the contributions from the intermediate states  $^3S_1(6s7s)$  and  $^3P_1(6p^2)$ , which totals to  $-21.78 \times 10^{-11}i(Q_W/N)ea_0$ . However, as mentioned earlier, the energy spacing of the important levels are not correct. In addition  $\langle ^3P_0(6s6p)||D||^3D_1(5d6s) \rangle$ ,  $\langle ^3P_0(6s6p)||D||^3S_1(6s7s) \rangle$  and  $|\langle 1S_0||D||1P_1 \rangle|$  also show variations from the experimental data and previous theoretical calculation[11]. Using the experimental excitation energies, the average of the experimental data of  $|\langle 1S_0||D||1P_1 \rangle|$ , and the other  $|D_{fi}|_s$  calculated by Porsev et al[11] gives  $-12.31 \times 10^{-10}i(Q_W/N)ea_0$ .

The contribution from the intermediate state  $^3D_1(5d6s)$  is  $-13.09 \times 10^{-10}i(Q_W/N)ea_0$  which is calculated using the reduced matrix element of  $\langle ^3D_1(5d6s)||H_{\text{PNC}}^{\text{NSI}}||^3P_0(6s6p) \rangle$  from the present work, the  $\langle ^1P_1(6s6p)||D||^3P_0(6s6p) \rangle$  from Porsev et al[11] and the energy denominator from the experimental data. The estimate of the  $\langle ^3D_1(5d6s)||H_{\text{PNC}}^{\text{NSI}}||^3P_0(6s6p) \rangle$  using the wave functions we have calculated is expected to be better as the magnetic dipole hyperfine structure

constant of  ${}^1P_1(6s6p)$  is in better agreement with the experimental data.

#### IV. CONCLUSIONS

Our MCDF calculations shows that the  $E1_{\text{PNC}}({}^3P_0(6s6p) - {}^1P_1(6s6p))$  PNC transition amplitude of  ${}^{171}\text{Yb}$  is more than two order of magnitude larger than that of the  $E1_{\text{PNC}}(6s - 7s)$ . Our calculation indicates the experimental proposal of Kimball[1] shows

that  ${}^3P_0(6s6p) - {}^1P_1(6s6p)$  is indeed a promising candidate for the  $E1_{\text{PNC}}$  measurements.

#### V. ACKNOWLEDGEMENTS

These calculations were done using the Enterprise450 at the Indian Institute of Astrophysics, Bangalore and the IBM workstations at the Physical Research Laboratory, Ahmedabad.

- 
- [1] D. F. Kimball. Phys. Rev. A **63**, 052113(2001).
- [2] C. S. Wood, S. C. Bennet, D. Cho, B. P. Masterson, J. L. Roberts, C. E. Tanner, and C. E. Wieman. Science **275**, 1559(1997).
- [3] S. A. Blundell, W. R. Johnson, and J. Sapirstein. Phys. Rev. Lett. **65**, 1411(1990).
- [4] V. A. Dzuba, V. V. Flambaum, and O. P. Sushkov. Phys. Lett. A **141**, 147(1989).
- [5] S. C. Bennet and C. E. Wieman. Phys. Rev. Lett **82**, 2484(1999).
- [6] W. J. Marciano and J. L. Rosner. Phys. Rev. Lett. **65**, 2963(1990).
- [7] A. Derevianko. Phys. Rev. Lett **85**, 1618(2000).
- [8] V. A. Dzuba, C. Harabati, and W. R. Johnson. Phys. Rev. A **63**, 044103(2001).
- [9] M. G. Kozlov, S. G. Porsev, and I. I. Tupitsyn. Phys. Rev. Lett **86**, 1607(2001).
- [10] Phys. Rev. A **56**,1635(1997).
- [11] S. G. Porsev, Yu. G. Rakhlina, and M. G. Kozlov. Phys. Rev. A **60**, 2781(1999).
- [12] S. G. Porsev, Yu G. Rakhlina, and M. G. Kozlov. JETP Lett. **61**, 459(1995).
- [13] David DeMille. Phys. Rev. Lett. **74**, 4165(1995).
- [27] C. J. Bowles, D. Budker, D. Commins, D. DeMille, S. J. Freedman, A. T. Nguyen, and S. Q. Shang. Phys. Rev. A **53**, 3103(1996).
- [15] C. J. Bowers, D. Budker, S. J. Freedman, G. Gwinner, J. E. Stalnaker, and D. DeMille. Phys. Rev. A **59**, 3513 (1999).
- [16] Angom Dilip Singh and Bhanu Pratap Das. Jour. of Phys. B **32**, 4905(1999).
- [17] K.G. Dyall, I.P. Grant, C.T. Johnson, F.A. Parpia, and E.P. Plummer. Compu. Phys. Comm. **55**, 425(1989).
- [18] V. A. Dzuba, V. V. Flambaum, and S. M. Ginges, Phys. Rev. A **63**,062101 (2001).
- [19] M. G. Kozlov and S. G. Porsev, Phys. Rev. A **64**, 052107 (2001).
- [20] V. A. Dzuba, V. V. Flambaum, and J. S. M. Ginges. Phys. Rev. A **61**, 062509 (2000).
- [21] Yu G Rakhlina S G Porsev y and M G Kozlov, *arXiv: physics/9810011*, (1998).
- [22] Ephraim Eliav and Uzi Kaldor, Phys. Rev. A, **52**, 2765 (1995).
- [23] O Topper, G H Gutohrlein, and P Hillermann, 1997 Abstracts of 29 EGAS (Berlin) 233.
- [24] Jin W-G et al, Journ. Phys. Soc. Jpn. **60** 2896 (1991).
- [25] J. Migdalek and W.E. Baylis, J. Phys. B **24**, L99 (1991).
- [26] M.D. Kunisz, Acta Phys. Pol. A **62**, 285 (1982).
- [27] C.J. Bowers, D. Budker, E.D. Commins, D. DeMille, S.J.Freedman, A.-T. Nguyen, and S.-Q. Shang, Phys. Rev. A **53**, 3103 (1996).
- [28] M. Baumann and G. Wandel, Phys. Lett. **22**, 283(1966).
- [29] N. P. Penkin, K. B. Blagoev, and V. A. Komarovskii, Atomic Physics VI, Riga, 1978, edited by R. Damburg Plenum Press, New York, 1978.
- [30] T. Andersen, O. Poulsen, P.S. Ramanujam, and A. Petrakiev-Petkov,Sol. Phys. **44**, 257 1975.